BJR

HIP

The histological and elemental characterisation of corrosion particles from taper junctions

S. Munir,
R. A. Oliver,
B. Zicat,
W. L. Walter,
W. K. Walter,
W. R. Walsh

Surgical and Orthopaedic Research Laboratory, Sydney, Australia

Objectives

This study aimed to characterise and qualitatively grade the severity of the corrosion particles released into the hip joint following taper corrosion.

Methods

The 26 cases examined were CoC/ABG Modular (n = 13) and ASR/SROM (n = 13). Blood serum metal ion levels were collected before and after revision surgery. The haematoxylin and eosin tissue sections were graded on the presence of fibrin exudates, necrosis, inflammatory cells and corrosion products. The corrosion products were identified based on visible observation and graded on abundance. Two independent observers blinded to the clinical patient findings scored all cases. Elemental analysis was performed on corrosion products within tissue sections. X-Ray diffraction was used to identify crystalline structures present in taper debris.

Results

The CoC/ABG Modular patients had a mean age of 64.6 years (49.4 to 76.5) and ASR/SROM patients had a mean age of 58.2 years (33.3 to 85.6). The mean time *in situ* for CoC/ABG was 4.9 years (2 to 6.4) and ASR/SROM was 6.1 years (2.5 to 8.1). The blood serum metal ion concentrations reduced following revision surgery with the exception of Cr levels within CoC/ABG. The grading of tissue sections showed that the macrophage response and metal debris were significantly higher for the ASR/SROM patients ($p < 0.001$). The brown/red particles were significantly higher for ASR/SROM ($p < 0.001$). The taper debris contained traces of titanium oxide, chromium oxide and aluminium nitride.

Conclusion

This study characterised and qualitatively graded the severity of the corrosion particles released into the hip joint from tapers that had corrosion damage.

Cite this article: *Bone Joint Res* 2016;5:370–378.

Keywords: Corrosion; Taper; Histology; Metal ion; Characterisation

Article focus

- Histological analysis of the tissue section due to corrosion in modular total hip arthroplasties.
- Determine potential changes corrosion particles have on tissue morphology.
- Identification and abundance of varying corrosion products found embedded within tissue sections.
- Corrosion particles were identified and graded on abundance in healthy tissue sections using colour.
- Understanding the oxides formed can determine the metallic ions which are present and determine the toxicity effects of both oxide formations and ions.

Key messages

- Characterised the corrosion products produced at taper junctions.

Strengths and limitations

- Patients were well matched in age and body mass index for both groups.
- There was a strict patient criteria.
- It was a small patient cohort.

S. Munir, MBioME, Biomedical Engineer,
R. A. Oliver, PhD, Research Fellow,
W. R. Walsh, PhD, Professor and director, Surgical and Orthopaedic Research Laboratory, Prince of Wales Clinical School Level 1, Clinical Science Bldg, Prince of Wales Hospital Gate 6 Avoca Street Sydney, 2031 Australia.
B. Zicat, Bsc, MD, CM, FRCSC, FRACS (Orth), FAOrthA, Orthopaedic Surgeon,
W. L. Walter, MBBS (Syd), FRACS (Orth), FAOrthA, PhD, Orthopaedic Surgeon,
W. K. Walter, MBBS (Syd), FRACS (Orth), FAOrthA, Orthopaedic Surgeon, Specialist Orthopaedic Group, Suite 1.08, Level One, 3 – 9 Gillies Street Wollstonecraft NSW 2065, Australia.

Correspondence should be sent to S. Munir; email: selin.munir@gmail.com

doi:10.1302/2046-3758.59.2000507

Bone Joint Res 2016;5:370–378.
Received: 27 July 2015;
Accepted: 24 May 2016

Introduction

The motivating drive behind better intra-operative implant positioning and semi-custom implants has resulted in a higher degree of complexity in modern stem design.[1-3] This design complexity is confounded by clinical concern stemming from the generation of metal wear debris and corrosion products from metal-on-metal (MoM) bearing articulations such as those at the femoral stem taper junctions found at both the head/stem, or within the femoral component.[4-6] Hip implant designs with multiple junctions include exchangeable neck, proximal shoulders, distal-stem, stem-sleeve and mid-stem junction components.[7,8] Designs with multiple taper junctions at the stem can have corrosion by-products or metal debris irrespective of having a ceramic-on-ceramic (CoC) bearing articulation. Clinical concerns relating to corrosion at taper junctions include local and systemic transfer of metal particles and corrosion debris, toxicity, inflammatory-like response in local tissues and fracture due to a weakened implant microstructure.[9-12] Corrosion was initially identified as dark staining on mating taper junctions with the dark discolouration of the surface reported as being corrosion by-products generated during the electrochemical process.[13-17]

Poor implant outcomes have been attributed to adverse reactions to metal debris (ARMD).[18,19] The histological changes observed in ARMD cases include a conglomerate of surface necrosis with macrophage response containing fine metallic particles. These histological findings also include granulomas in the presence of perivascular lymphocytic infiltrate with or without germinal centres.[20] The possible degradation products generated from bearing wear or corrosion are either free metallic ions, inorganic metal salts, metal-protein complexes, or metal oxides.[21] Analysis of the corrosion products is limited in the literature, with only a few studies reporting on the type of products produced during corrosion which are found at the taper junction.[17,21,22] One study has shown different foreign particles embedded in tissue sections of patients who have had corrosion at the taper junction, however, a detailed analysis of these particles has not yet been conducted.[22]

This study examined the corrosion products present in tissue samples from a cohort of patients implanted with a CoC articulation and a taper junction as well as patients with a MoM articulation and a taper junction. Specific identification of the crystalline structures found within the debris will provide confirmation of the chemical state of each metal species and the effects these particles have on local tissues.

Patients and Methods

Surgical procedure. Human ethics approval was obtained from St Vincent's Human Research Ethics Committee (File 09/123) covering the collection of human tissue during surgery for research purposes. Tissue samples were collected between February 2010 and February 2014, inclusive, from the affected hip joints intra-operatively. Tissue sections were collected at regions that were exposed to the implant within the hip joint capsule. The collection protocol was to obtain tissue that appeared necrotic or to obtain tissue in regions where dark staining was found around the taper junctions of the implant. Once collected, the tissue sections were placed in formalin.

Implant component and patient selection. Patient selection criteria required a unilateral hip arthroplasty that underwent revision surgery due to metal-related symptoms. It also required a complete set of metal ion levels consisting of cobalt (Co) and chromium (Cr) in blood serum, explants, radiographs and tissue samples. The reason for consultation commonly seen across the patient cohort was groin pain and limited mobility of the hip joint. After applying the selection criteria, two stem designs with a total of 26 cases were included in this study. Group 1 was a CoC bearing with an ABG Modular stem (Stryker, Mahwah, New Jersey) and group 2 was a MoM bearing with an SROM stem (DePuy, Warsaw, Indiana). Group 1 cohort was made up of 13 patients that were selected from an initial pool of 30. Group 2 cohort was made up of 13 patients that were selected from an initial pool of 20. The ABG Modular stem is manufactured from a titanium alloy (Ti-Mn-Zn-Fe) with a cobalt alloy (Co-Cr-Mo) exchangeable neck. Patients implanted with an ABG Modular femoral component were paired with a fourth generation CeramTec BIOLOX delta ceramic femoral head (Ceramtec, Plochingen, Germany) ranging from 28 mm to 36 mm in size. The SROM stem is manufactured from a titanium alloy (Ti-6Al-4V). Patients implanted with a SROM femoral component were paired with a XL Total ASR MoM femoral head (DePuy) ranging from 39 mm to 51 mm in size. The CoC/ABG Modular system can only present corrosion damage at the neck-stem taper junction whilst the ASR/SROM system has both the bearing articulation and two taper junctions which can contribute to both metal wear debris and corrosion products.

Metal ion collection. Pre- and post-operative metal ion collection was conducted using a pre-established protocol.[23] Pre-operative blood serum metal ion levels used in this study were collected at an average time of 3.4 months (1.4 to 20.1) for group 1, and 4.1 months (0.3 to 22.8) months for group 2, before revision surgery. Post-operative blood serum metal ion levels used in this study were collected at a mean of 1.5 months (0.03 to 3.3) months for group 1, and 6.2 months (0.3 to 17.6) for group 2 after revision surgery. Cup inclination and anteversion were measured on the anteroposterior (AP) radiographs using the Ein-Bild-Roentgen-Analyse (EBRA) software by one reviewer who knew which implant they were grading but was blinded to the study criteria.[24]

Tissue sectioning and grading. Tissue blocks were harvested at the time of surgery and categorised as capsular

Table I. A modified grading system to assess the tissue morphological changes to metal-related pathology[25-27]

Group and grading	Description
Synovial lining	
Type 1 surface	Intact synovial surface epithelium
Type 2 surface	Loss of synoviocyte layer without fibrin deposition
Type 3 surface	Fibrin deposition
Type 4 surface	Extensive necrosis with loss of architecture
Necrosis	(Necrosis is graded only for tissue sections that were graded with a Type 4 surface for the synovial lining)
Grade 1	Tissue necrosis resulted in the loss of synoviocyte
Grade 2	Less than 25% of the tissue showed extensive necrosis with loss of architecture, or tissue presented with fibrin deposition
Grade 3	The tissue section presented with tissue necrosis between 25% to 75% in addition to loss in architecture
Grade 4	The tissue section presented tissue necrosis > 75% in addition to loss of architecture
Cellularity	
Macrophages	
Grade 0	Macrophages were absent
Grade 1	Occasional macrophages were seen within the tissue section
Grade 2	Macrophages were observed in clusters within the tissue section
Grade 3	The tissue contained diffuse/sheets of macrophages
Lymphocytes	
Grade 0	No lymphocytes
Grade 1	Diffuse synovitis
Grade 2	Lymphoid aggregate synovitis
Grade 3	Germinal centre containing synovitis
Metallic particles	
Grade 0	Granules absent
Grade 1	Barely discernible at ×250, easily confirmed at ×400
Grade 2	Discrete granules resolved at ×100
Grade 3	Discrete granules resolved at ×25
Grade 4	Masses visible at ×10

Table II. The grading system to assess the abundance of the different corrosion particles found embedded within tissue sections

Group and grading	Description
Corrosion product colour identification	
Green (shards)	
Grade 0	Absent
Grade 1	Occasional
Grade 2	Clusters
Grade 3	Abundant
Brown/black	
Grade 0	Absent
Grade 1	Occasional
Grade 2	Clusters
Grade 3	Abundant
Brown/red	
Grade 0	Absent
Grade 1	Occasional
Grade 2	Clusters
Grade 3	Abundant

tissue, deep hip tissue, or granuloma tissue. Tissue samples were placed into histology cassettes and embedded in paraffin. All slides were de-waxed in xylene before being stained using a Harris haematoxylin and eosin (H & E) stain. Between two and five tissue sections were examined per case. Stained tissue sections were graded under an Olympus BX43 optical light microscope (Olympus, Tokyo, Japan) using a minimum of 10× magnification. For macrophage detection or lower traces of metal debris, higher magnifications of 20× to 40× were used. Two blinded independent observers scored all cases. The tissue grading for the haematoxylin and eosin tissue sections evaluated the presence of fibrin exudates, necrosis, inflammatory cells and metallic deposits shown in Table I.[20,22,25-27]

A binary system was used to identify the presence of the corrosion products. If present, the particles were assessed by abundance (Table II). The cumulative score of all tissue sections was used to determine the final scores.

Scanning electron microscope and energy-dispersive x-ray spectroscopy. Samples with a grade 3 result were selected to further analysis of the corrosion products and to further identify the different particles graded within the tissue. Figure 1 represents the three types of corrosion particles detected in the tissue sections. A scanning electron microscope (SEM) Hitachi S3400 (Hitachi, Tokyo, Japan) was used in backscatter mode to identify any metallic particles embedded within the tissue sections identified in the histology slides. Energy-dispersive x-ray spectrum (EDS) analysis was used to provide the elemental composition of the particles found within the tissue samples. This method was previously used to analyse ceramic debris and it has been extended to analyse metal particles.[28]

X-ray diffraction. Taper debris was collected at the taper junction from all (n = 26) of the retrieved implants intraoperatively. Care was taken to not contaminate the debris with blood. Following collection, the taper debris collected from each individual case (n = 13 per group) was combined into one single sample and crushed into fine particles using a ceramic mortar and pestle for each group. Once the debris was crushed, it was placed into two separate collection tubes labelled CoC/ABG Modular and MoM/SROM. A X'pert multipurpose X-ray diffraction system (PANanalytical, Egham, United Kingdom) obtained a spectrum of the taper debris for each group. The selected setting for the mask slit controlling the irradiated width of the sample was ten. The selected input parameters using the X'Pert Data Collector software for both groups were: start angle set at 20°; final angle set at 95°; step size was 0.026°; and time per step was 499.80°/second. Each spectrum obtained was analysed against the elemental composition of its femoral stem. The metal elements searched for in the CoC/ABG Modular group were titanium (Ti), cobalt (Co), chrome (Cr), molybdenum (Mo), iron (Fe), manganese (Mn) and zinc (Zn). The etal elements searched for in the MoM/SROM taper debris were: Ti, Aluminium (Al), Vadium (V), Co, Cr, and Mo. The second analysis conducted analysed only the three major elements based on the highest percent composition within the metal alloys. For the ABG Modular

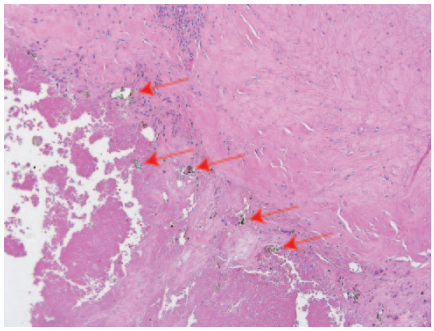

Fig. 1a

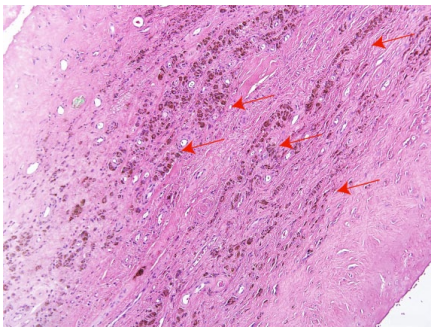

Fig. 1b

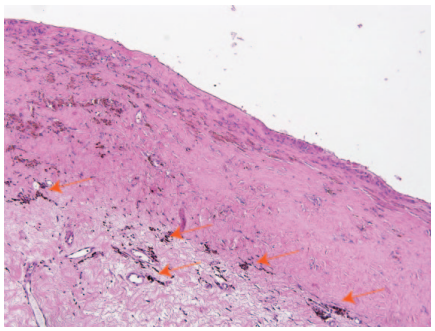

Fig. 1c

Histological images showing a) a low-power photomicrograph representing a score of 3 for green shards found within the tissue. The tissue section illustrates an abundance of green shards indicated by blue arrows within the section; b) a low-power photomicrograph representing a score of 3 for brown/red coloured corrosion particles found within the tissue. The tissue section illustrates an abundance of brown/red coloured corrosion particles indicated by blue arrows within the section; and c) a low-power photomicrograph representing a score of 3 for brown/black coloured corrosion particles found within the tissue. The tissue section illustrates an abundance of brown/black coloured corrosion particles indicated by blue arrows within the section.

Table III. The results of the patient demographics for both group 1 and group 2 with the relevant p-value where statistical analysis was conducted

Demographics	Group 1	Group 2	p-value
Hips (n)	13	13	-
Age (yrs)	64.6 (49.4 to 76.5)	58.2 (33.3 to 85.6)	0.21
Gender ratio	4M:10F	6M:7F	-
Femoral head size	32 mm (28 to 40)	45 mm (39 to 55)	< 0.05
Bearing	CoC	MoM	-
Femoral stem	ABG Modular	SROM	-
Time *in situ* (yrs)	4.9 (2.0 to 6.4)	6.1 (2.5 to 8.1)	0.07
Mean BMI (kg/m²)	27.9	27.7	0.94

The Mann-Whitney U test was used as the statistical test used to determine the p-value for the age, time *in situ*, head size and BMI
CoC, ceramic on ceramic; MoM, metal on metal; BMI, body mass index

group this was Ti, Co, and Cr. For the SROM group, it was Co, Cr, and Ti.

Statistical analysis. All statistical analysis was conducted using the SPSS statistical software package (SPSS Inc., Chicago, Illinois). The Mann-Whitney U test was used to assess the differences for non-normally distributed data. For continuous variables the means and standard deviations (SD) were given and comparison between groups was conducted using independent samples *t*-tests. Categorical variables were reported in percentages and compared between groups using the chi-squared test. The chosen confidence interval of 95% returned a significance level of 0.05, therefore a p-value < 0.05 was considered to be significant.

Results

Clinical analysis. The patient demographics for the cohort are presented in Table III. Radiological follow-up of all patients showed well fixed and well positioned implants in consecutive films with no radiolucent lines at two years post-operatively.

The mean inclination and anteversion angles for CoC/ABG Modular patients were 49.4° (SD 4.5°) and 21.1° (SD 3.8°), respectively. The mean inclination and anteversion angles for MoM/SROM patients were 43.7° (SD 5.4°) and 19.6° (SD 5.4°), respectively.

Table IV. The mean blood serum metal ion levels for cobalt, chromium, and titanium in parts per billion for group 1 on the left and the mean metal ion levels for cobalt and chromium for group 2 on the right. The last column shows the corresponding p-value obtained after statistical analysis

Metal ions in serum	Group 1	Group 2	p-value
Number of patients	13	13	
Mean cobalt (Co) level pre-operatively	6.22 (2.24 to 11.15)	13.19 (1.30 to 26.20)	0.01
Mean cobalt (Co) level post-operatively	2.17 (0.29 to 6.55)	1.43 (0.65 to 3.07)	0.23
Mean chromium (Cr) level pre-operatively	1.12 (0.52 to 2.08)	7.36 (0.73 to 20.28)	0.001
Mean chromium (Cr) level post-operatively	1.01 (0.52 to 1.46)	2.21 (1.01 to 4.47)	0.001
Mean titanium (Ti) level pre-operatively	4.26 (1.91 to 6.70)	Not collected	-
Mean titanium (Ti) level post-operatively	3.82 (2.39 to 6.70)	Not collected	-

The Mann-Whitney U test was used to determine the p-value of the patient metal ion levels

Metal ion levels. Table IV presents the mean pre- and post-revision metal ion levels for both groups.

The Co (p = 0.001) and Cr (p = 0.02) levels significantly reduced after revision surgery for the MoM/SROM patients. CoC/ABG Modular patients showed a significant reduction (p = 0.0002) in the Co, however, the decrease of Cr ion concentration was not statistically significant (p = 0.48).

Grading of corrosion products. The mean grades for the corrosion products are shown in Figure 2. The presence of brown/red particles was significantly higher (p < 0.001) in the MoM/SROM group compared with the CoC/ABG Modular group. The MoM/SROM group had 73% of the tissue sections embedded with corrosion debris in comparison with 20% found within the CoC/ABG Modular group. The CoC/ABG Modular patients had double the amount of green fragments (20%) embedded

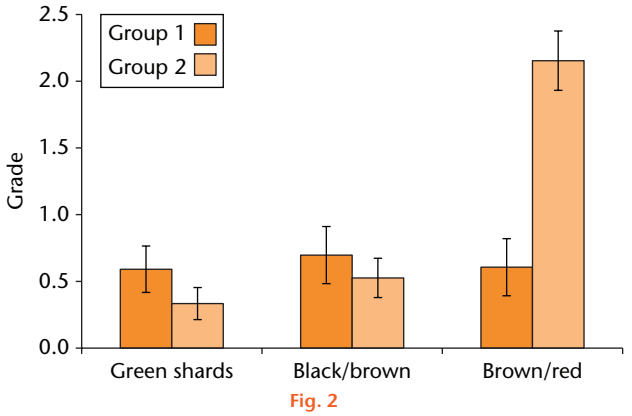

Fig. 2

The scores for the three different corrosion particles found for each group. The mean grades from both groups are represented where blue identifies group 1 and red identifies group 2.

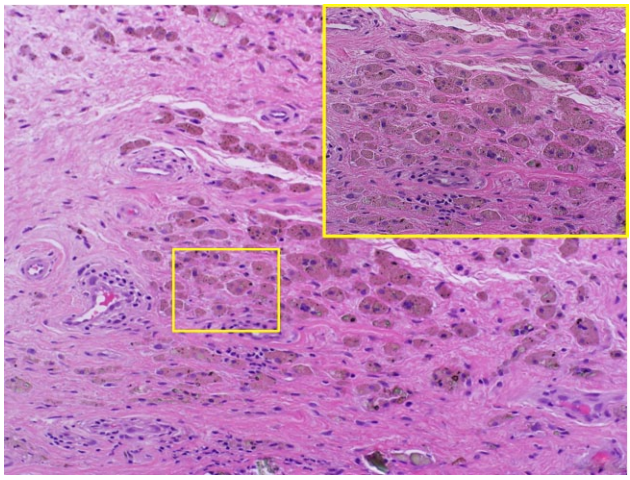

Fig. 3a

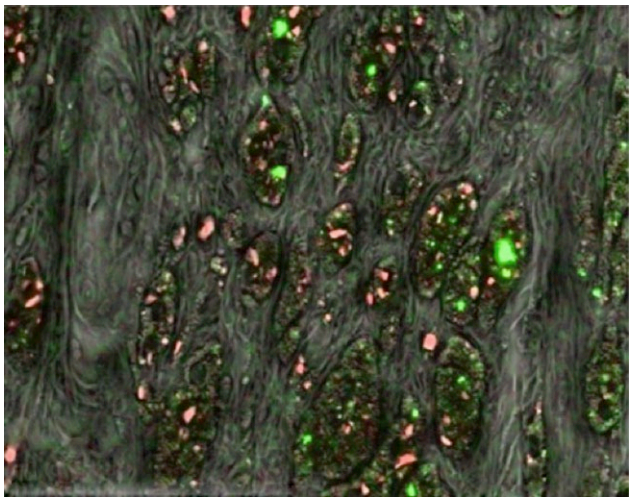

Fig. 3b

A histological section that has a) foreign particles embedded within the tissue. The foreign particles of interest are represented as brown-reddish in appearance; and b) a mapped region of the SEM used to identify the elemental species present in the tissue where Cr is shown in red and Ti particles in green.

within tissue specimens compared with the MoM/SROM group (10%), although this difference was not statistically significant ($p = 0.19$).

The green fragments were generally present in smaller aggregates in comparison with the larger shards found within CoC/ABG Modular patients. The brown/black particles were found more commonly within the CoC/ABG Modular group where 25% of the tissue sections were graded with the presence of brown/black particles in comparison to 18% of tissue sections within the MoM/SROM group ($p = 0.50$). The different geometry and colour of the debris present within both groups indicates the potential for different composition of the metallic products as a result of the varying stages within the corrosion process or different processes altogether.

SEM/EDS of corrosion products. The brown/red globular regions were observed across the tissue samples for both groups. Elemental analysis detected that the brown/red globular regions contained evenly scattered Ti (green) and Cr (red) particles as shown in Figure 3. The green shards showed chromium as a major metallic element with traces of cobalt also detected (Fig. 4). The black/brown particles from CoC/ABG Modular patients showed that the dominant metallic element was Ti, however, Fe and Cr were also detected.

XRD of corrosion debris. X-Ray diffraction analysis revealed the crystalline structures with a strong correlation to the CoC/ABG Modular elemental profile. The debris consisted of iron titanium oxide, cobalt oxide, and chromium oxide. The identification of these elements is presented in Figure 5. The secondary analysis of the major metallic elements of the femoral stem revealed peaks matching the following crystalline structures: chromium oxide (CrO), titanium oxide (TiO_2), and chromium oxide (Cr_2O_3). The XRD analysis revealed that the crystalline structures with a strong correlation to the MoM/SROM taper debris were aluminium nitride (AlN) and chromium oxide (Cr_2O_3), as shown in Figure 6. The secondary analysis of the major elements revealed the same crystalline structures.

Tissue histology. The grading results from the tissue sections were compared between the CoC/ABG Modular and ASR/SROM groups and are shown in Figure 7. Both implant configurations produced an advance local tissue response observed from the graded tissue sections. Tissue necrosis showed no significant difference ($p > 0.05$) between the two groups, however, the CoC/ABG Modular patients had a higher recorded level of necrosis. The metallic particles were significantly more abundant ($p = 0.05$) within the MoM/SROM group at 78% in comparison with the CoC/ABG Modular group at 50%. The macrophage response to foreign particles between the two groups varied significantly ($p = 0.006$) with group 2 (MoM/SROM) having higher scores.

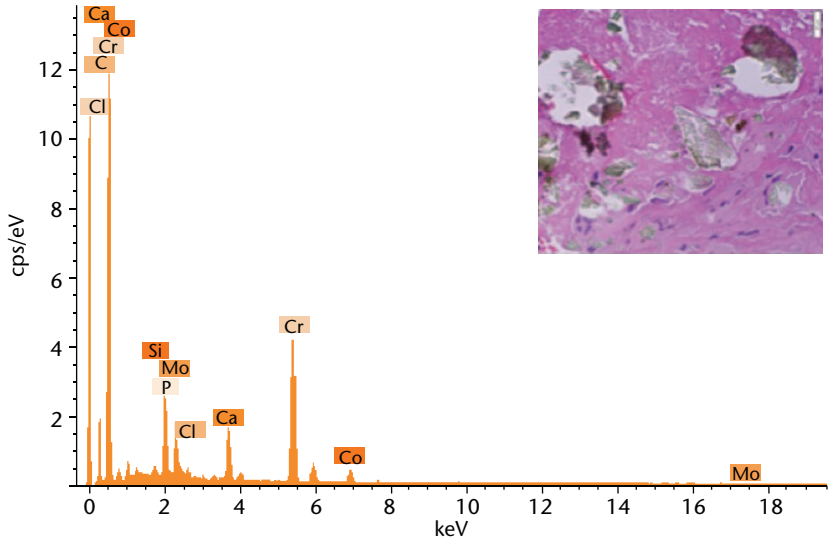

Fig. 4

Energy-dispersive x-ray spectrum of the green coloured fragments embedded within the tissue sections as shown in the previous figure by a blue arrow.

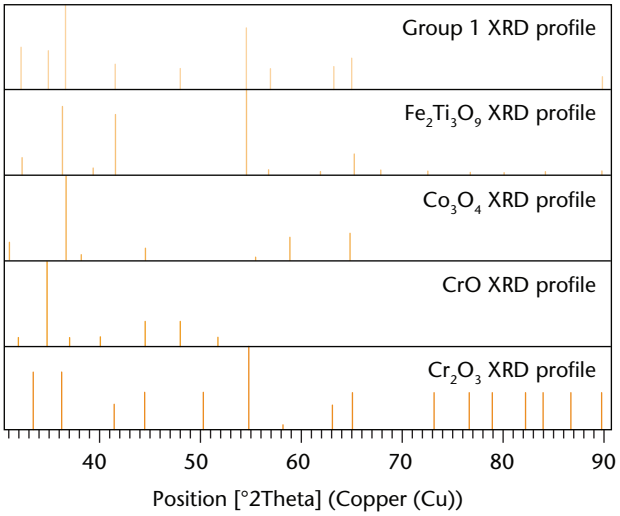

Fig 5

XRD spectrum of the taper debris collected from group 1 patients shown as the top profile (orange). The elemental profiles of crystalline structure were matched with possible candidates present within the taper debris. The surface profiles are ranked on scores with $Fe_2Ti_3O_9$ (blue), Co_3O_4 (green), CrO (grey), Cr_2O_3 (brown).

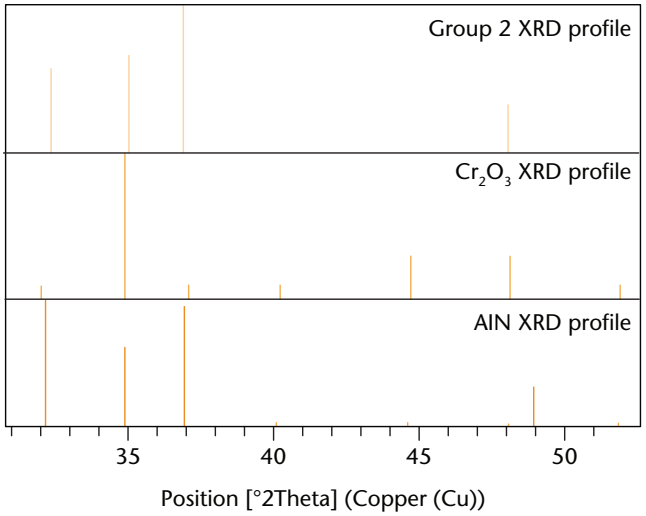

Fig 6

XRD spectrum of the taper debris collected from group 2 patients shown as the top profile (orange). The elemental profiles of crystalline structure were matched with possible candidates present within the taper debris. The surface profiles are ranked on scores with Co_3O_4 (blue), and AlN (green).

Discussion

This study was conducted using revision patients diagnosed for metal-related symptoms, therefore the numbers used within the study were limited to the largest cohorts found which could be a control group (exclude metal bearing wear) and a 'worst case' group (both bearing wear and taper corrosion). The former group will only have a corroded taper to provide identification of the corrosion particles released into the hip joint. This will allow a direct comparison with corrosion debris. However, the small number used in this study is a limiting factor due to potential variations of corrosion found on the implant and the severity of the tissue damage amongst patients. This can lead to an increase in the standard error within the study.

Understanding corrosion from taper junctions is of significant clinical importance. Huber et al[29] showed dominant peaks in Cr, P, and O, however, no Co was observed using

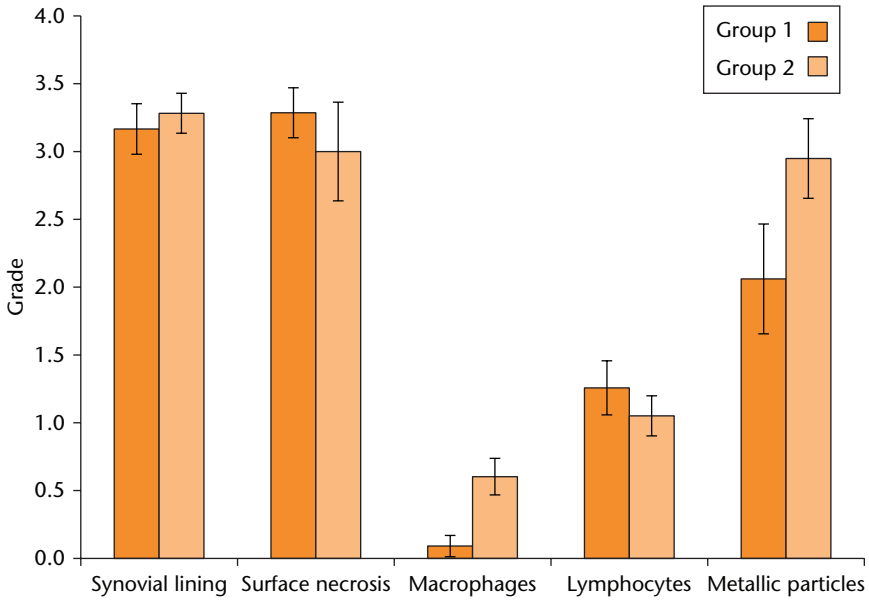

Fig 7

The grading scores for tissue morphological changes. Each category assessed is represented for both groups.

EDX; this agrees with the conducted analysis on the corrosion particles. The presence of phosphate detected using elemental analysis concurs with other findings that report on $CrPO_4$, suggesting that its presence can be limited or formed within the tissue and be absent in the debris.[26] However, the debris did not find any traces of $CrPO_4$.

The EDX analysis of the CoC/ABG Modular tissue sections found traces of Ti, Cr and Fe that are specific to the material composition of the Stryker stem. The presence of Fe in the EDX analysis for this specific stem has not been reported before. The detection of iron in the tissue indicates that patients will have Fe ions released from the implant. Similarly, the XRD profile from the taper debris collected from the CoC/ABG Modular group showed a combination of ZrO_2, $Fe_2Ti_3O_9$, CO_3O_4, and Cr_2O_3. The detection of these chemical compounds within the taper debris identifies the presence of local corrosion and the products embedded in the tissue surrounding the affected hip joint.[22,30,31] The crystalline structure identified for titanium within the CoC/ABG group was $Fe_2Ti_3O_9$ which has a brown to black colour, indicating that the Ti ions are commonly bound to iron and oxygen molecules and appear in an oxidised form within the tissue.[32] The presence of ZrO_2 is most likely from the ceramic bearing. The detection of ceramic particles within the taper debris can be a potential source of aggressive fretting within the junction, leading to premature failure of the implant if ceramic particles are present at the taper junction. Titanium oxide (TiO_2), has a tetragonal crystal structure, and is a metallic alloy with a reddish brown colour.[33,34] The finding of red/brown particles for both groups indicates that the taper junctions are corroding and Ti metal ions are released from the taper junctions. The presence of TiO_2 is also a confirmation that the oxide layer is removed during the cyclic activity by fretting and metal ions are released into the local tissue where they further oxidise.

An interesting finding when grading the green "shard-like" fragments was that they did not always associate with a cellular response. Large fragments were found within the tissue with no inflammatory-like response surrounding the foreign particle. EDX analysis of the green shards embedded across tissue sections from both groups presented strong traces of Cr and Co. A recent study conducted on tissue sections of implants has reported finding green fragments within tissue sections, however, EDX analysis has not been previously reported on the specific products.[22] A study conducted by Jacobs et al[17] reports on the presence of pale green fragments that are translucent, agreeing with the EDX results, which detected the presence of Cr, Co, and P. The combination of XRD and EDS characterises the green fragments within the tissue sections and taper debris as Cr_2O_3.

Exchangeable neck implant designs have seen early failure rates, suggesting the aggressive formation of corrosion at the distal taper junction.[4,31,35,36] The more distal taper connection and a greater angle to the femoral axis can produce greater loading and micromovement within this junction, causing more aggressive fretting and resulting in accelerated corrosion. The formation of Cr_2O_3 products can only be a result of taper corrosion and not related to metal wear debris from the bearing as the CoC/ABG Modular group only has a MoM articulation at the second taper junction.

The metal ions of Co and Cr are cytotoxic, with studies showing that ions and reactive oxygen species released by cobalt, chromium and chromium orthophosphates activate the immune system.[10,37-40] This can relate to the

high level of necrosis observed and inflammatory-like response seen in local tissue sections. High levels of Cr ions have been reported for resurfacings due to bearing wear, which can be a potential reason for the higher level of Cr seen in the MoM/SROM group compared with the CoC/ABG group.[41] The metal ion valance for the assessed Cr ions found within blood serum analysis is most likely to be Cr^{2+} or Cr^{3+} which have a lower toxicity to humans in comparison with the highly toxic Cr^{6+}.[39,40] The XRD data that identified the corrosion particles as Cr_2O_3 suggest that the ionic species of chromium in the tissue is Cr^{3+}. This finding is supported by the abundance of green shards found in the tissue and taper debris surrounding the CoC/ABG Modular implant.

Histopathological studies focusing on MoM bearings have commonly reported small black metal debris within the tissue sections resultant of bearing wear.[37,42,43] The taper debris XRD profile collected from the MoM/SROM patients closely resembled the profile of Cr_2O_3 and AlN. The presence of these two crystalline structures is indicative of corrosion at the taper junction rather than metal transfer given that aluminium is only present within the stem material.

Histological examination of the tissue from both groups showed similar findings regarding corrosion products, inflammatory reaction, and tissue pathology, which is similar to other studies focusing on specific implant design.[31,44-46] As with other study findings, the level of synoviocyte loss was high for both groups with both presenting extensive tissue necrosis.[31,46] Surprisingly, the necrosis was graded higher in MoM/SROM patients, which conflicts with intra-operative findings of severe necrotic tissue in the ABG/Modular patients.[47] Other implant-specific studies have shown higher levels of necrosis within tissue sections.[31,48,49] The possible reason for the lack of macrophages within the CoC/ABG Modular group tissue sections can be attributed to the large regions of necrosis found in tissue samples, which prevented grading of cellular activity. The higher detection of brown/red particles in the tissue sections of the MoM/SROM patients is due to the higher number of sources with a potential to increase metal wear debris. However, considering the red/brown particles consisted of both Ti and Cr debris and are also present in the CoC/ABG Modular group, this does not indicate that they originate from the articular bearing surface.

This study has characterised the corrosion products produced by corrosion processes at the taper junction. Tissue architecture showed similar changes in both groups although a higher abundance of corrosion products produced a greater macrophage response.

References

1. **Noble PC, Box GG, Kamaric E, et al.** The effect of aging on the shape of the proximal femur. *Clin Orthop Relat Res* 1995;316:31-44.
2. **Noble PC, Alexander JW, Lindahl LJ, et al.** The anatomic basis of femoral component design. *Clin Orthop Relat Res* 1988;235:148-165.
3. **Dunbar MJ.** The proximal modular neck in THA: a bridge too far: affirms. *Orthopedics* 2010;33:640.
4. **Matsushita A, Nakashima Y, Fujii M, Sato T, Iwamoto Y.** Modular necks improve the range of hip motion in cases with excessively anteverted or retroverted femurs in THA. *Clin Orthop Relat Res* 2010;468:3342-3347.
5. **Srinivasan A, Jung E, Levine BR.** Modularity of the femoral component in total hip arthroplasty. *J Am Acad Orthop Surg* 2012;20:214-222.
6. **Molloy DO, Munir S, Jack CM, et al.** Fretting and corrosion in modular-neck total hip arthroplasty femoral stems. *J Bone Joint Surg [Am]* 2014;96-A:488-493.
7. **McTighe LK.** Thomas Tkach, Historical Review of Stem Modularity. In: McTighe T, ed. Reference Book on Total Hip Modularity. Joint Implant Surgery & Research Foundation; 2008.
8. **Carangelo RJ, Bono JV.** Modularity in total hip arthroplasty: the S-ROM Prosthesis. In: *Revision Total Hip Arthroplasty*. New York: Springer Verlag, 1999:224-233.
9. **Werner SD, Bono JV, Nandi S, Ward DM, Talmo CT.** Adverse tissue reactions in modular exchangable neck implants: a report of two cases. *J Arthroplasty* 2013 28:543.e13-15.
10. **Polyzois I, Nikolopoulos D, Michos I, Patsouris E, Theocharis S.** Local and systemic toxicity of nanoscale debris particles in total hip arthroplasty. *J Appl Toxicol* 2012;32:255-269.
11. **Bernstein M, Desy NM, Petit A, et al.** Long-term follow-up and metal ion trend of patients with metal-on-metal total hip arthroplasty. *Int Orthop* 2012;36:1807-1812.
12. **De Smet K, De Haan R, Calistri A, et al.** Metal ion measurement as a diagnostic tool to identify problems with metal-on-metal hip resurfacing. *J Bone Joint Surg [Am]* 2008;90-A(Suppl 4):202-208.
13. **Agins HJ, Alcock NW, Bansal M, et al.** Metallic wear in failed titanium-alloy total hip replacements. A histological and quantitative analysis. *J Bone Joint Surg [Am]* 1988;70-A:347-356.
14. **Mathiesen EB, Lindgren JU, Blomgren GG, Reinholt FP.** Corrosion of modular hip prostheses. *J Bone Joint Surg [Br]* 1991;73-B:569-575.
15. **Collier JP, Surprenant VA, Jensen RE, Mayor MB.** Corrosion at the interface of cobalt-alloy heads on titanium-alloy stems. *Clin Orthop Relat Res* 1991;271:305-312.
16. **Collier JP, Surprenant VA, Jensen RE, Mayor MB, Surprenant HP.** Corrosion between the components of modular femoral hip prostheses. *J Bone Joint Surg [Br]* 1992;74-B:511-517.
17. **Jacobs JJ, Urban RM, Gilbert JL, et al.** Local and distant products from modularity. *Clin Orthop Relat Res* 1995;319:94-105.
18. **Cooper HJ, Della Valle CJ, Berger RA, et al.** Corrosion at the head-neck taper as a cause for adverse local tissue reactions after total hip arthroplasty. *J Bone Joint Surg [Am]* 2012;94-A:1655-1661.
19. **Fricka KB, Ho H, Peace WJ, Engh CA Jr.** Metal-on-metal local tissue reaction is associated with corrosion of the head taper junction. *J Arthroplasty* 2012;27(8 Suppl):26-31.e1.
20. **Natu S, Sidaginamale RP, Gandhi J, Langton DJ, Nargol AV.** Adverse reactions to metal debris: histopathological features of periprosthetic soft tissue reactions seen in association with failed metal on metal hip arthroplasties. *J Clin Pathol* 2012;65:409-418.
21. **Jacobs JJ, Hallab NJ, Skipor AK, Urban RM.** Metal degradation products: a cause for concern in metal-metal bearings? *Clin Orthop Relat Res* 2003;417:139-147.
22. **Perino G, Ricciardi BF, Jerabek SA, et al.** Implant based differences in adverse local tissue reaction in failed total hip arthroplasties: a morphological and immunohistochemical study. *BMC Clin Pathol* 2014;14:39.
23. **Tai SM, Millard N, Munir S, et al.** Two-year serum metal ion levels in minimally invasive total conservative hip resurfacing: preliminary results of a prospective study. *ANZ J Surg* 2015;85:164-168.
24. **Ochsner PE.** Measurement of the acetabular migration by using standard AP radiographs (EBRA): technique, results and practical application in clinical work. *J Bone Joint Surg [Br]* 1998;80-B:33.
25. **Davies AP, Willert HG, Campbell PA, Learmonth ID, Case CP.** An unusual lymphocytic perivascular infiltration in tissues around contemporary metal-on-metal joint replacements. *J Bone Joint Surg [Am]* 2005;87-A:18-27.
26. **Davda K, Lali FV, Sampson B, Skinner JA, Hart AJ.** An analysis of metal ion levels in the joint fluid of symptomatic patients with metal-on-metal hip replacements. *J Bone Joint Surg [Br]* 2011;93-B:738-745.
27. **Willert HG, Buchhorn GH, Fayyazi A, et al.** Metal-on-metal bearings and hypersensitivity in patients with artificial hip joints. A clinical and histomorphological study. *J Bone Joint Surg [Am]* 2005;87-A:28-36.
28. **Esposito C, Maclean F, Campbell P, et al.** Periprosthetic tissues from third generation alumina-on-alumina total hip arthroplasties. *J Arthroplasty* 2013;28:860-866.

29. **Huber M, Reinisch G, Trettenhahn G, Zweymüller K, Lintner F.** Presence of corrosion products and hypersensitivity-associated reactions in periprosthetic tissue after aseptic loosening of total hip replacements with metal bearing surfaces. *Acta Biomater* 2009;5:172-180.
30. **Xia Z, Kwon YM, Mehmood S, et al.** Characterization of metal-wear nanoparticles in pseudotumor following metal-on-metal hip resurfacing. *Nanomedicine* 2011;7: 674-681.
31. **Cooper HJ, Urban RM, Wixson RL, Meneghini RM, Jacobs JJ.** Adverse local tissue reaction arising from corrosion at the femoral neck-body junction in a dual-taper stem with a cobalt-chromium modular neck. *J Bone Joint Surg [Am]* 2013;95-A:865-872.
32. **Grey IE, Watts JA.** Mineralogical nomenclature: pseudorutile revalidated and neotype given. *Mineral Mag* 1994;58:597-600.
33. **Devilliers D, Dinh MT, Mahé E, Fatouros N.** Behaviour of titanium in sulphuric acid - application to DSAs. *J New Mater Electrochem Syst* 2006;9:221-232.
34. **Lener EF.** *Mineral Chemistry of Heavy Minerals in the Old Hickory Deposit, Sussex and Dinwiddie Counties, Virginia*. Blacksburg, Virginia: Virginia Tech, 1997.
35. **Gill IP, Webb J, Sloan K, Beaver RJ.** Corrosion at the neck-stem junction as a cause of metal ion release and pseudotumour formation. *J Bone Joint Surg [Br]* 2012;94-B:895-900.
36. **Srinivasan A, Jung E, Levine BR.** Modularity of the femoral component in total hip arthroplasty. *J Am Acad Orthop Surg* 2012;20:214-222.
37. **Billi F, Campbell P.** Nanotoxicology of metal wear particles in total joint arthroplasty: a review of current concepts. *J Appl Biomater Biomech* 2010; 8:1-6.
38. **Bradberry SM, Wilkinson JM, Ferner RE.** Systemic toxicity related to metal hip prostheses. *Clin Toxicol (Phila)* 2014;52:837-847.
39. **Simonsen LO, Harbak H, Bennekou P.** Cobalt metabolism and toxicology–a brief update. *Sci Total Environ* 2012;432:210-215.
40. **Germain MA, Hatton A, Williams S, et al.** Comparison of the cytotoxicity of clinically relevant cobalt-chromium and alumina ceramic wear particles in vitro. *Biomaterials* 2003;24:469-479.
41. **Vendittoli PA, Roy A, Mottard S, et al.** Metal ion release from bearing wear and corrosion with 28 mm and large-diameter metal-on-metal bearing articulations: a follow-up study. *J Bone Joint Surg [Br]* 2010;92-B:12-19.
42. **Amstutz HC, Le Duff MJ.** Background of metal-on-metal resurfacing. *Proc Inst Mech Eng H* 2006;220:85-94.
43. **Langton DJ, Jameson SS, Joyce TJ, et al.** Early failure of metal-on-metal bearings in hip resurfacing and large-diameter total hip replacement: A consequence of excess wear. *J Bone Joint Surg [Br]* 2010;92-B:38-46.
44. **Toni A, Sudanese A, Paderni S, et al.** Cementless hip arthroplasty with a modular neck. *Chir Organi Mov* 2001;86:73-85. (In Italian)
45. **Kop AM, Swarts E.** Corrosion of a hip stem with a modular neck taper junction: a retrieval study of 16 cases. *J Arthroplasty* 2009;24:1019-1023.
46. **Gill IP, Webb J, Sloan K, Beaver RJ.** Corrosion at the neck-stem junction as a cause of metal ion release and pseudotumour formation. *J Bone Joint Surg [Br]* 2012;94-B:895-900.
47. **Hallab NJ, Jacobs JJ.** Biologic effects of implant debris. *Bull NYU Hosp Jt Dis* 2009;67:182-188.
48. **Campbell P, Ebramzadeh E, Nelson S, et al.** Histological features of pseudotumor-like tissues from metal-on-metal hips. *Clin Orthop Relat Res* 2010;468:2321-2327.
49. **Milošev L, Antolič V, Minovič A, et al.** Extensive metallosis and necrosis in failed prostheses with cemented titanium-alloy stems and ceramic heads. *J Bone Joint Surg [Br]* 2000;82-B:352-357.

Funding Statement

- W. R. Walter reports funding received from Stryker, MatOrtho and Norton Rose; W. K. Walter reports funding received from Global Orthopaedic Technology, and B. Zicat reports funding received from DePuy, none of which is related to this article.

Author Contributions

- S. Munir: Design of study, Writing of manuscript.
- R. A. Oliver: Histology result analysis, Review of manuscript.
- B. Zicat: Assistance with clinical discussion, Review of results and manuscript.
- W. L. Walter: Review of manuscript.
- W. K. Walter: Assistance with clinical discussion, Review of results.
- W. R. Walsh: Review of manuscript, Discussion of results.

ICMJE conflict of interest

- None declared